Nanoscale

Cite this: *Nanoscale*, 2011, **3**, 4560

www.rsc.org/nanoscale

COMMUNICATION

A multiplexed separation of iron oxide nanocrystals using variable magnetic fields†

John T. Mayo,[a] Seung Soo Lee,[a] Cafer T. Yavuz,[a] William W. Yu,[a] Arjun Prakash,[b] Joshua C. Falkner[a] and Vicki L. Colvin*[a]

Received 24th June 2011, Accepted 21st August 2011
DOI: 10.1039/c1nr10671f

The size-dependent magnetic properties of nanocrystals are exploited in a separation process that distinguishes particles based on their diameter. By varying the magnetic field strength, four populations of magnetic materials were isolated from a mixture. This separation is most effective for nanocrystals with diameters between 4 and 16 nm.

Many technologies have been developed for nanoscale iron oxides, including MRI imaging,[1] water purification,[2,3] on-demand drug delivery,[4] and cell culture transfection.[5] In the latter examples, the motive response of magnetic particles to external fields is central to their application. Even modest magnetic fields, on the order of millitesla, can be sufficient to concentrate nanocrystals from suspensions.[6] Such separations can be useful in minimal infrastructure settings for water purification.[7] Alternatively, in biological separations magnetic separation can result in the capture and release of nanoparticles and their cargo.[8]

There are various methods of fine size separation for nanomaterials including centrifugation,[9] salts-based size-selective precipitation,[10] size exclusion chromatography,[11] and diafiltration,[12] but these processes do not take advantage of the magnetic properties demonstrated by iron oxide nanoparticles. The magnetic separation of coated nanoscale iron oxides and a binary form of magnetic chromatography has previously been demonstrated by Moeser *et al.*[13] Here, we expand upon these standard approaches to magnetic separation by using varying field strengths which separate different particles based on their diameter. The process does not simply separate nanoparticles based on whether they move in response to a magnetic field; rather, it separates nanocrystals based on the magnitude of their response to applied fields. Thus, several different populations can be separated from a complex mixture, in what we term here a 'multiplexed' separation in analogy to a multiplexed analysis.[14] This capability is particularly critical for biotechnology where it is often desirable to separate more than one type of component from a complex mixture.[15–17] Alternatively, in the present example it enables the size distribution of magnetic nanocrystals to be sharpened using a method that is effective, fast, and consumes minimal solvent.

This multiplex separation scheme is based on the premise that as the magnetic field acting on a nanoparticle suspension is increased, the concentrated particle residues becomes enriched in smaller particles.[6,18] This enrichment reflects the size-dependent behavior of the particles: as compared to larger (*e.g.* d > 15 nm) particles, smaller diameter nanocrystals require larger magnetic fields in order to move at room temperature. The size dependence has been the subject of some study.[6,19,20] It is generally thought that in an external magnetic field, nanocrystals may reversibly aggregate and align their magnetic dipoles. This is due to the fact that the particle sizes in question are superparamagnetic and, therefore, experience large magnetizations in the presence of magnetic fields while retaining no magnetization upon the removal of the external field.[19] The forces required to move particles of this size range within a magnetic separator require reversible aggregation, and are dependent on particle size, concentration, and magnetic Bjerrum length, which is explicitly detailed by De Las Cuevas *et al.*[19] The larger structures would have very large magnetic moments, and in an external magnetic field would experience substantial motive force.[6] The tendency for superparamagnetic materials to aggregate is expected to increase with particle size due, in part, to larger magnetic susceptibilities.[19] In addition, Bégin-Colin and co-workers indicate that smaller sizes of iron oxide crystals are enriched in the less magnetic maghemite (γ-Fe_2O_3) as opposed to magnetite (Fe_3O_4) which may also contribute to their reduced response to external fields.[20]

To evaluate whether these known size-dependent properties could be the basis for a multiplexed magnetic separation, we prepared four different sizes of iron oxide nanocrystals *via* the thermal decomposition of iron oleate.[21,22] Specific reaction details can be found in the supplemental materials.† Excess reactants in the as-prepared samples were removed by repeated cycles of flocculation upon ethanol and acetone addition, followed by centrifugation. The supernatant was then decanted and the precipitated particles were redispersed in a small quantity of hexanes (Aldrich, certified ACS grade). This process was repeated several times, and the resulting black suspensions were stored in hexanes with no evidence of aggregation over months. These iron oxide samples were very uniform, and had

[a]*Rice University, Chemistry, 6500 Main Street, Houston, Texas, 77030, United States. E-mail: colvin@rice.edu; Fax: +713-348-2578; Tel: +713-348-5741*
[b]*Rice University, Chemistry and Biomolecular Engineering, 6500 Main Street, Houston, Texas, 77030, United States; Fax: +713-348-2578; Tel: +713-348-5741*

† Electronic supplementary information (ESI) available. See DOI: 10.1039/c1nr10671f

average diameters of 4.0 ± 0.4, 9.2 ± 1.0, 11.7 ± 1.1, and 15.9 ± 1.4 nm (see Supplementary Fig. S1†).

The size-dependent response of these individual particles to an applied external field is shown in Fig. 1. This data was obtained using a conventional high gradient magnetic separator (HGMS) (see Supplementary Fig. S2†). This device applies a large external field to a narrow column (6.3 mm ID) filled with stainless steel wool; the steel wool creates regions of high field gradients which serve to collect magnetic particles. While the exact values of the magnetic gradients are difficult to calculate in this geometry, they do scale with increasing applied field.[23,24] For these studies, the particles were suspended in hexanes and gravity fed (~1 min) through the 22.3 cm long column. The effluent thus contained nanoparticles not captured by a particular applied field; the retained material could be recovered by removing the field and washing the column with additional hexanes. Quantitative analysis of the iron content of the starting suspensions and the effluent allowed for the calculation of the percent nanoparticles retained at varying applied magnetic fields.

Fig. 1 shows the percent of nanoparticles retained in the column as external field strengths were increased from millitesla to 1.6 T. As expected, the smallest particles were the least retained by the column. Even at field strengths as high as 1.6 T (not shown), less than 17% of the material was captured by the column. In contrast the larger particles were almost completely retained (98%) at only 0.23 T. The intermediate diameters exhibited retention characteristics between the large and small extremes. This data suggests that at specific applied fields (vertical lines in Fig. 1) it is possible to selectively retain larger diameter nanocrystals.

The four sizes of nanoscale iron oxides were then combined (Fig. 2) to form a multimodal sample with distinct populations of iron oxide. The diameters of these materials were different enough to be distinguished by transmission electron microscopy (TEM) as illustrated by the colored circles in Fig. 2. This mixed sample was passed through an HGMS subjected to a very small external field (0.05 T). As expected from Fig. 1, the largest iron oxide particles (15.9 nm) were retained in the column. The magnetic field was then turned off, and

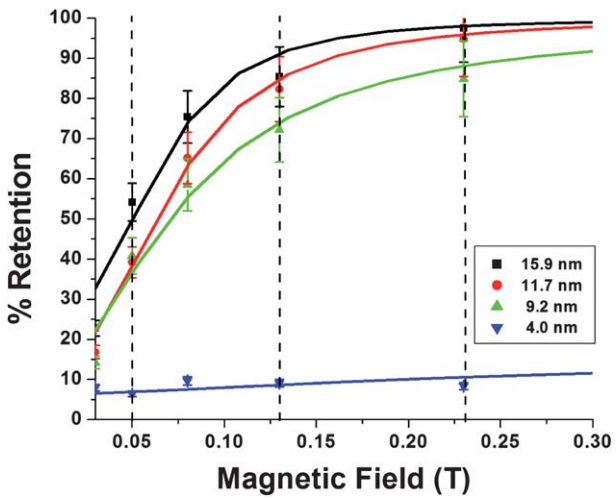

Fig. 1 These data illustrate the magnetic field required to retain the nanoscale iron oxide samples at specific particle diameters. This plot was utilized to determine the magnetic fields necessary for the tetramodal magnetic separation. Magnetic field strengths used in this experiment are marked with dashed lines.

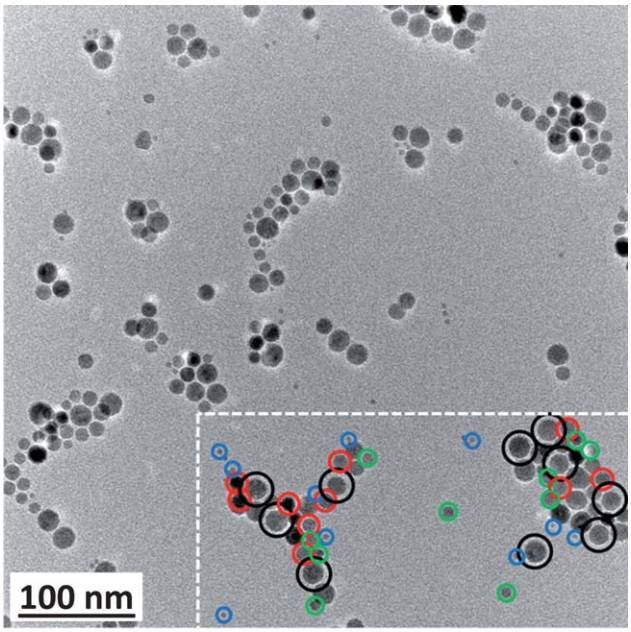

Fig. 2 TEM images of mixed tetramodal iron oxide nanocrystal sample produced by quantitatively mixing four monodisperse iron oxide samples. In the dashed box, selected particles are circled to indicate their size: black for the 15.9 nm particles, red for the 11.7 nm particles, green for the 9.2 nm particles, and blue for the 4.0 nm particles.

the column was flushed with hexanes to collect the largest nanocrystals. The effluent from the HGMS at 0.05 T was then run through the HGMS at 0.13 T; at this field strength we expected the second largest iron oxide particles (11.7 nm) to be preferentially retained in the column. After collecting this material from the column, the procedure was repeated at 1.59 T to retain 9.2 nm particles, and the 4.0 nm particles were isolated in the effluent. The magnetic field was

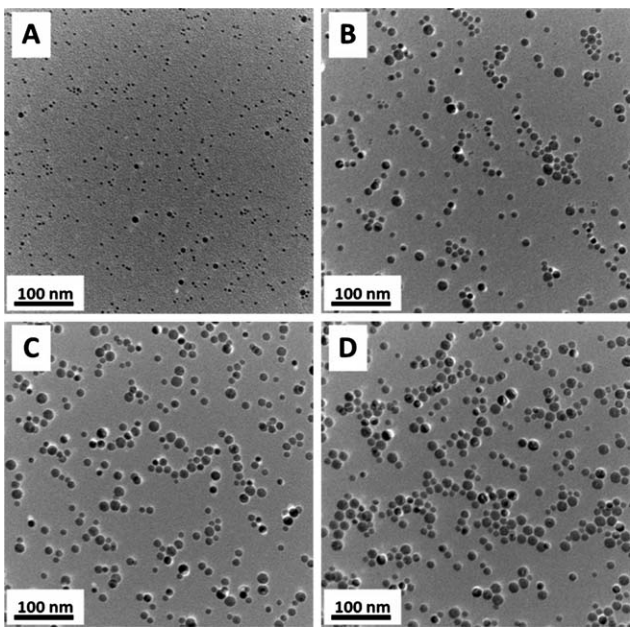

Fig. 3 TEM images of iron oxide samples obtained (a) at 1.59 T, (b) at 0.23 T, (c) at 0.13 T, and (d) at 0.05 T.

then reduced to 0.23 T and the 9.2 nm sample was rinsed out. Each of the four collected samples were analyzed by TEM (Fig. 3). The resulting particle size distributions, shown in Fig. 4, were determined using Image Pro sizing software.

Fig. 4 shows that it is possible to separate nanoparticles based on size using variable field applications; however, as is apparent in the data that the larger nanocrystals do not separate as well as the smaller materials. For example, in just one pass through the column the smallest size (4.0 nm) is separated relatively cleanly; fewer than 16% of the material in this sample contained the larger sizes. In contrast, at lower field strengths the resulting effluents show an enrichment in a particular particle size rather than a complete separation. Such data is consistent with Fig. 1 as well which shows the differences in response to applied magnetic fields is less pronounced as particle sizes increase. These observations result from the fact that the magnetic properties of these materials change most drastically when diameters fall below 27 nm.[25] This is in part due to the fact that for isolated particles, the magnetic moment decreases with diameter.[20] Iron oxide nanoparticles have been shown to form chains under the influence of an applied magnetic field.[26] Additionally, linear or network aggregation of larger particles may occur even without an external magnetic field.[27] This could prematurely induce aggregation which would make it more difficult to distinguish larger particles based on their isolated or non-aggregated diameters.

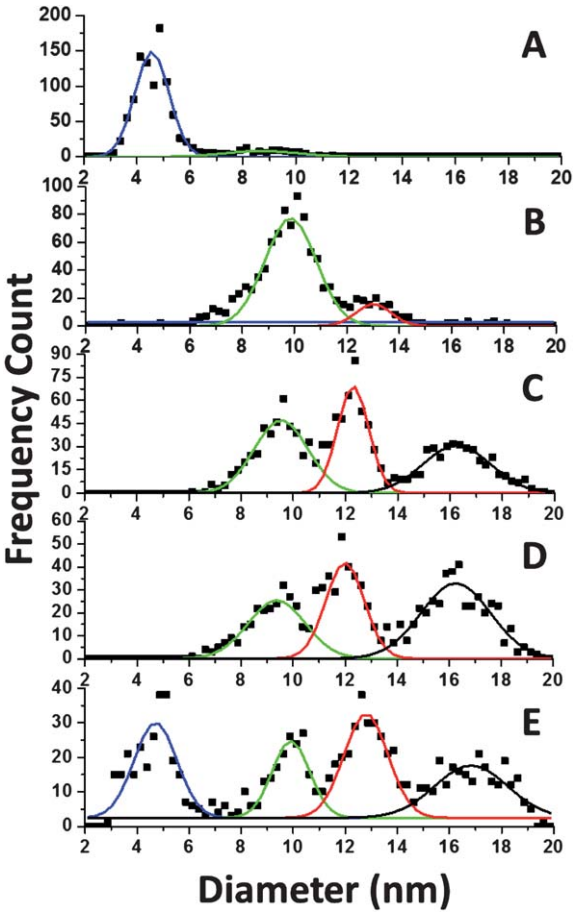

Fig. 4 Distributions of nanocrystal diameters for the iron oxide samples obtained (a) at 1.59 T, (b) at 0.23 T, (c) at 0.13 T, (d) at 0.05 T, and (e) the starting tetramodal iron oxide sample.

This variable field separation does not immediately lead to a baseline separation of particles under the conditions studied; rather, the process creates samples that are enriched in particular particle diameters. To quantify this enrichment as a function of diameter, we calculated the separation efficiency from the purity of the recovered materials. We defined the relative abundance, R, in a separated sample as:

$$R = \frac{F}{1 - F} \tag{1}$$

where F is the fraction of iron oxide nanocrystals within a specified diameter range. The enrichment factor, α, was then found from:

$$\alpha = \frac{R_f}{R_i} \tag{2}$$

where R_i and R_f, are the relative abundance of the desired diameter range before and after magnetic separation, respectively.[28] For the experiments performed here, we achieved enrichment factors of 18.7 for diameters ranging from 1 to 5.5 nm; 6.7 for diameters from 5.5 to 10.5 nm; 1.8 for diameters from 10.5 to 13.5 nm; and 1.7 for diameters greater than 13.5 nm. The enrichment factors for all size ranges were greater than one, implying that productive enrichment is taking place.

These enrichment factors can also be used to estimate the performance of a variable-field magnetic separation under more optimized conditions. Enrichment processes often rely on separations which are applied multiple times. In this case, one may envision longer HGMS columns, or alternatively successive exposure of samples to the same magnetized column. Because little material remains in the column after it is demagnetized the product yields per pass are quite high, making multiple treatments practical. For smaller samples, it is possible to achieve a relative abundance of 9, or 90% purity, through only two applications of the column (or twice as long of column). In contrast, six successive column passes are required in order to ensure 90% pure samples of the two larger particles.

The data presented here provides a novel example of a size-dependent magnetic multiplex separation of iron oxide nanocrystals. A distinct trend in separation was observed with diameter, and this could be applied to separate different sizes from a mixture using a conventional HGMS column. Small sizes could be separated quite effectively, yielding an 84% pure sample. In principle, more highly purified nanocrystal populations can be recovered either by using longer columns, or by relying on successive passes through the standard columns. In nanomanufacturing, this separation could be applied to sharpen the size distribution of non-uniform materials as well as separate particles from the solvents and surfactants used in preparation. In biological applications which conventionally use magnetic beads, a variable field separation with appropriately designed particle diameters could be used to separate more than one cell type or biomolecule from complex mixtures.

Conclusions

In summary, the size-dependent properties of magnetic nanocrystals can be used as the basis for a variable field separation. We report for the first time the use of this principle for the enrichment of particular particle diameters in a complex mixture of four distinct diameter populations. The separation is particularly effective for distinguishing very small (*e.g.* 4 nm) from larger (*e.g.* > 12 nm) nanocrystals.

Acknowledgements

We thank NSF for its support of the Center for Biological and Environmental Nanotechnology (EEC-0647452). We also acknowledge with gratitude the Office of Naval Research (N00014-04-1-0003), and the U.S. Environmental Protection Agency Star Program (RD-83253601-0) for funding. J.T.M. thanks the Robert A. Welch Foundation (C-1342) for a graduate fellowship.

References

1 J. Qin, S. Laurent, Y. S. Jo, A. Roch, M. Mikhaylova, Z. M. Bhujwalla, R. N. Muller and M. Muhammed, *Adv. Mater.*, 2007, **19**, 1874–1878.
2 J. T. Mayo, C. Yavuz, S. Yean, L. Cong, H. Shipley, W. Yu, J. Falkner, A. Kan, M. Tomson and V. L. Colvin, *Sci. Technol. Adv. Mater.*, 2007, **8**, 71–75.
3 S. Yean, L. Cong, C. T. Yavuz, J. T. Mayo, W. W. Yu, A. T. Kan, V. L. Colvin and M. B. Tomson, *J. Mater. Res.*, 2011, **20**, 3255–3264.
4 T. Hoare, J. Santamaria, G. F. Goya, S. Irusta, D. Lin, S. Lau, R. Padera, R. Langer and D. S. Kohane, *Nano Lett.*, 2009, **9**, 3651–3657.
5 H. Y. Zhang, M. Y. Lee, M. G. Hogg, J. S. Dordick and S. T. Sharfstein, *ACS Nano*, 2010, **4**, 4733–4743.
6 C. T. Yavuz, J. T. Mayo, W. W. Yu, A. Prakash, J. C. Falkner, S. Yean, L. L. Cong, H. J. Shipley, A. Kan, M. Tomson, D. Natelson and V. L. Colvin, *Science*, 2006, **314**, 964–967.
7 C. T. Yavuz, J. T. Mayo, C. Suchecki, J. Wang, A. Z. Ellsworth, H. D'Couto, E. Quevedo, A. Prakash, L. Gonzalez, C. Nguyen, C. Kelty and V. L. Colvin, *Environ. Geochem. Health*, 2010, **32**, 327–334.
8 M. Franzreb, M. Siemann-Herzberg, T. J. Hobley and O. R. T. Thomas, *Appl. Microbiol. Biotechnol.*, 2006, **70**, 505–516.
9 J. A. Jamison, K. M. Krueger, C. T. Yavuz, J. T. Mayo, D. LeCrone, J. J. Redden and V. L. Colvin, *ACS Nano*, 2008, **2**, 311–319.
10 C.-L. Wang, M. Fang, S.-H. Xu and Y.-P. Cui, *Langmuir*, 2010, **26**, 633–638.
11 A. M. Al-Somali, K. M. Krueger, J. C. Falkner and V. L. Colvin, *Anal. Chem.*, 2004, **76**, 5903–5910.
12 S. F. Sweeney, G. H. Woehrle and J. E. Hutchison, *J. Am. Chem. Soc.*, 2006, **128**, 3190–3197.
13 G. D. Moeser, K. A. Roach, W. H. Green, T. A. Hatton and P. E. Laibinis, *AIChE J.*, 2004, **50**, 2835–2848.
14 G. D. Liu, J. Wang, J. Kim, M. R. Jan and G. E. Collins, *Anal. Chem.*, 2004, **76**, 7126–7130.
15 A. Agrawal, T. Sathe and S. M. Nie, *J. Agric. Food Chem.*, 2007, **55**, 3778–3782.
16 B. I. Haukanes and C. Kvam, *Bio-Technology*, 1993, **11**, 60–63.
17 S. Bucak, D. A. Jones, P. E. Laibinis and T. A. Hatton, *Biotechnol. Prog.*, 2003, **19**, 477–484.
18 J. S. Beveridge, J. R. Stephens, A. H. Latham and M. E. Williams, *Anal. Chem.*, 2009, **81**, 9618–9624.
19 G. De Las Cuevas, J. Faraudo and J. Camacho, *J. Phys. Chem. C*, 2008, **112**, 945–950.
20 A. Demortiere, P. Panissod, B. P. Pichon, G. Pourroy, D. Guillon, B. Donnio and S. Begin-Colin, *Nanoscale*, 2011, **3**, 225–232.
21 J. Park, K. J. An, Y. S. Hwang, J. G. Park, H. J. Noh, J. Y. Kim, J. H. Park, N. M. Hwang and T. Hyeon, *Nat. Mater.*, 2004, **3**, 891–895.
22 W. W. Yu, J. C. Falkner, C. T. Yavuz and V. L. Colvin, *Chem. Commun.*, 2004, 2306–2307.
23 A. Ditsch, S. Lindenmann, P. E. Laibinis, D. I. C. Wang and T. A. Hatton, *Ind. Eng. Chem. Res.*, 2005, **44**, 6824–6836.
24 M. R. Parker, *Phys. Technol.*, 1981, **12**, 263–268.
25 M. Ma, Y. Wu, H. Zhou, Y. K. Sun, Y. Zhang and N. Gu, *J. Magn. Magn. Mater.*, 2004, **268**, 33–39.
26 S. Z. Malynych, A. Tokarev, S. Hudson, G. Chumanov, J. Ballato and K. G. Kornev, *J. Magn. Magn. Mater.*, 2010, **322**, 1894–1897.
27 K. Butter, P. H. H. Bomans, P. M. Frederik, G. J. Vroege and A. P. Philipse, *Nat. Mater.*, 2003, **2**, 88–91.
28 A. S. Krass, P. Boskma, B. Elzen and W. A. Smit, *Uranium Enrichment and Nuclear Weapon Proliferation*, Taylor & Francis Ltd, London, 1983.